

# Enhancing $thj$ Production from Top-Higgs FCNC Couplings

Lei Wu

*ARC Centre of Excellence for Particle Physics at the Terascale,  
School of Physics, The University of Sydney, NSW 2006, Australia*

(Dated: July 31, 2018)

## Abstract

In this paper, we study the single top and Higgs associated production  $pp \rightarrow thj$  in the presence of top-Higgs FCNC couplings ( $\kappa_{tqh}, q = u, c$ ) at the LHC. Under the current constraints, we find that the cross section of  $pp \rightarrow thj$  can be sizably enhanced in comparison with the SM predictions at 8 and 14 TeV LHC. We also find that the full cross section of  $pp \rightarrow thj$  with  $\kappa_{tch}$  is larger than the resonant cross section of  $pp \rightarrow t\bar{t} \rightarrow thj$  by a factor 1.16 at 8 TeV LHC and 1.12 at 14 TeV LHC, respectively. We further explore the observability of top-Higgs FCNC couplings through  $pp \rightarrow t(\rightarrow b\ell^+\nu_\ell)h(\rightarrow \gamma\gamma)j$  and find that the branching ratios  $Br(t \rightarrow qh)$ ,  $Br(t \rightarrow uh)$  and  $Br(t \rightarrow ch)$  can be respectively probed to 0.12%, 0.23% and 0.26% at  $3\sigma$  sensitivity at 14 TeV LHC with  $\mathcal{L} = 3000 \text{ fb}^{-1}$ .

PACS numbers: 14.65.Ha,14.80.Ly,11.30.Hv

## I. INTRODUCTION

The discovery of the Higgs boson at the LHC is a great triumph of the Standard Model(SM) and marks a new era in the particle physics [1, 2]. Given the large uncertainties of the current Higgs data, there remains a plenty of room for new physics in Higgs sector [3]. So the precise measurement of the Higgs boson's properties will be a dominant task at the LHC in the next decades.

Concerning the probe of new physics through the Higgs boson, the Yukawa couplings can play the important role since they are sensitive to new flavor dynamics beyond the SM. In particular, top quark, as the heaviest SM fermion, owns the strongest Yukawa coupling and has the preference to reveal the new interactions at the electroweak scale [4]. One of the interesting things is that the top quark is just heavier than the observed Higgs boson, which makes the top quark flavor changing neutral current(FCNC) processes  $t \rightarrow hq$  ( $q = u, c$ ) be accessible in kinematics. In the SM, these top quark FCNC transitions are extremely suppressed by the G.I.M. mechanism [5]. But they can be greatly enhanced by the extended flavor structures in many new physics models, for example the minimal supersymmetric model (MSSM) with/without R-parity [6, 7], two-Higgs-doublet model(2HDM) type-III [8, 9], and the other miscellaneous models [10–12]. So the study of top-Higgs FCNC interactions is a common interest of the theory and experiment communities [13–16]. However, up to now, the null results of the searches for  $t \rightarrow qh$  at the LHC give the strong limits on the top-Higgs FCNC couplings. Among them, the most stringent constraint  $Br(t \rightarrow hc) < 0.56\%$  at 95% C.L. was reported by the CMS collaboration from a combination of the multilepton channel and the diphoton plus lepton channel [16]. Except for the widely studied  $t \rightarrow qh$  decays, the importance of the single top+Higgs production  $pp \rightarrow th$  in probing the top-Higgs FCNC couplings has been also emphasized in the recent theoretical studies [17–22].

In this paper, we investigate the top-Higgs FCNC interactions through  $pp \rightarrow thj$  with the sequent decays  $t \rightarrow b\ell^+\nu$  and  $h \rightarrow \gamma\gamma$  at the LHC. In the SM, the process  $pp \rightarrow thj$  can only be induced by the weak charged current interaction and has a relative small cross section, which is about 18 (88) fb at 8 (14) TeV LHC. However, such a process is found to be very sensitive to modifications of the Higgs couplings [23–30]. In particular, the top-Higgs FCNC couplings  $tqh(q = u, c)$  can sizably enhance  $thj$  cross section due to the contributions from the strong interaction processes. To be specific, there are mainly three new kinds of processes

that can contribute to the production of  $thj$  at the LHC: (1) gluon fusion  $gg \rightarrow thj$ , it is the dominant contribution, as shown in Fig.1, where  $hj$  can be produced not only by an on-shell top quark but also by an off-shell top quark via the new flavor changing couplings  $tqh$ ; (2)  $q\bar{q}$  fusion  $q\bar{q} \rightarrow thj$ , as shown in Fig.2, which is the sub-leading contribution. However, such a process is affected by the initial Parton Distributions Functions(PDFs). So one can use this feature to disentangle the FCNC couplings of the top quark with light quarks; (3)  $q\bar{q}$  annihilation  $q\bar{q} \rightarrow thj$ , which is similar to the  $s$ -channel of the process  $gg \rightarrow thj$  but with  $q\bar{q}$  instead of  $gg$  in the initial states. The contribution of this process is relatively smaller than (1) and (2) because of the suppression of color factor and PDFs; Based on the above considerations, it is worthwhile to perform a complete calculation of  $pp \rightarrow thj$  in the presence of the top-Higgs FCNC couplings by including the contributions (1)-(3), and explore its sensitivity to probe the top-Higgs FCNC couplings at the LHC.

This paper is arranged as follows. In Sec. II, we set up the notations and briefly describe the top-Higgs FCNC interactions. In Sec. III, we discuss the observability of the top-Higgs FCNC couplings through the process  $pp \rightarrow thj$  at 14 TeV LHC. Finally, a summary is given in Sec. IV.

## II. TOP-HIGGS FCNC INTERACTIONS

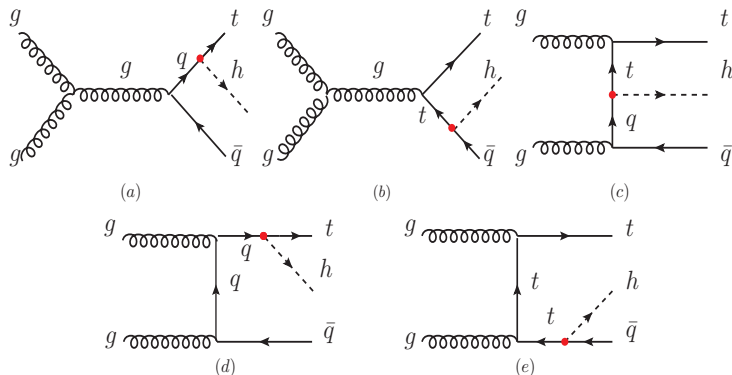


FIG. 1: Example Feynman diagrams for the partonic process  $gg \rightarrow th\bar{q}$  at the LHC through flavor violating top-Higgs interactions in Eq.(1)(marked with red dots). Here  $q = u, c$ .

A general effective Lagrangian describing the top-Higgs FCNC interaction can be written as

$$-\mathcal{L}_{tqh} = \kappa_{tqh}^L \bar{t}_L q_R h + \kappa_{tqh}^R \bar{t}_R q_L h + h.c.. \quad (1)$$

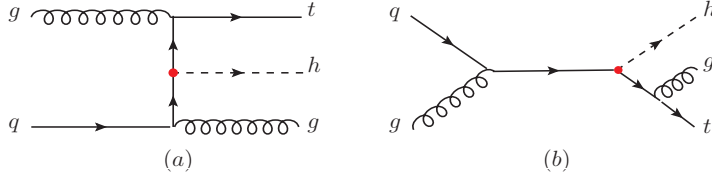


FIG. 2: Example Feynman diagrams for the partonic process  $qg \rightarrow thg$  at the LHC through flavor violating top-Higgs interactions in Eq.(1)(marked with red dots). Here  $q = u, c$ .

where  $h$  is the SM Higgs boson, and the real parameter  $\kappa_{tqh}^{L,R}$  denote the left-handed and right-handed FCNC couplings of the Higgs boson to the light up-type quarks  $q = u, c$ . We plot example Feynman diagrams in Fig.1 and Fig.2 for the partonic process  $gg \rightarrow th\bar{q}$  and  $qg \rightarrow thg$ , respectively. Some diagrams of the process  $u\bar{u}/d\bar{d} \rightarrow th\bar{q}$  can be obtained by replacing the initial gluons with  $u\bar{u}/d\bar{d}$  in the  $s$ -channel in Fig.1. By neglecting the light quark masses and assuming the dominant top decay width  $t \rightarrow bW$ , the Leading Order(LO) branching ratio of  $t \rightarrow qh$  can be approximately given by,

$$Br(t \rightarrow qh) = \frac{\kappa_{tqh}^{L^2} + \kappa_{tqh}^{R^2}}{2\sqrt{2}m_t^2 G_F} \frac{(1 - x_h^2)^2}{(1 - x_W^2)^2 (1 + 2x_W^2)}. \quad (2)$$

where  $G_F$  is the Fermi constant,  $x_W = m_W/m_t$  and  $x_h = m_h/m_t$ . The NLO QCD correction to  $Br(t \rightarrow qh)$  is estimated as 10% according to the results of high order corrections to  $t \rightarrow bW$  [31] and  $t \rightarrow ch$  [32]. In some specific models, the left-handed coupling  $\kappa_{tqh}^L$  is not expected to be large because its relation with the CKM mixing parameter. Also,  $\sqrt{\kappa_{tqh}^{L^2} + \kappa_{tqh}^{R^2}}$  can be constrained by the low energy observables, such as  $B^0 - \bar{B}^0$  mixing [9, 33]. However, we do not consider these indirect constraints in our study since they are model-dependent and their relevance strongly depends on the assumptions made for the generation of the quark flavor structures [34]. On the other hand, the CMS collaboration reported a model-independent bound  $\sqrt{\kappa_{tqh}^{L^2} + \kappa_{tqh}^{R^2}} < 0.14$  at 95% C.L. from the combined result of multilepton and diphoton in  $t\bar{t}$  production [16], which indicates  $|\kappa_{tqh}^{L,R}|$  should be less than 0.14. In our work, we assume  $\kappa_{tqh}^L = \kappa_{tqh}^R = \kappa_{tqh}$  and require  $\kappa_{tqh} \leq 0.1$  to satisfy the direct constraint from the CMS result.

### III. NUMERICAL CALCULATIONS AND DISCUSSIONS

We implement the top-Higgs FCNC interactions by using the package FeynRules [35] and calculate the LO cross section of  $pp \rightarrow thj$  with MadGraph5 [36]. We use CTEQ6L

as the parton distribution function(PDF) [37] and set the renormalization scale  $\mu_R$  and factorization scale  $\mu_F$  to be  $\mu_R = \mu_F = (m_t + m_h)/2$ . The SM input parameters are taken as follows [38]:

$$\begin{aligned} m_t &= 173.07 \text{ GeV}, & m_Z &= 91.1876 \text{ GeV}, & \alpha(m_Z) &= 1/127.9, \\ \sin^2 \theta_W &= 0.231, & m_h &= 125 \text{ GeV}, & \alpha_s(m_Z) &= 0.1185. \end{aligned} \quad (3)$$

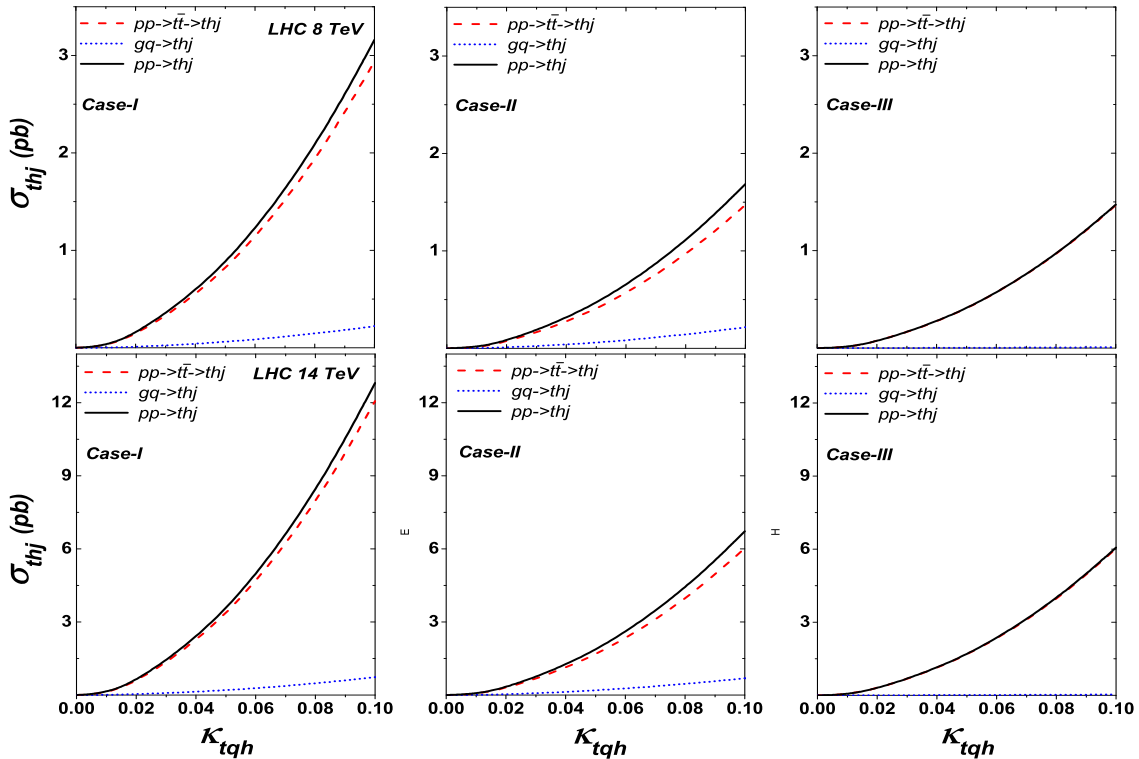


FIG. 3: The dependence of the cross sections  $\sigma_{thj}$  at 8 and 14 TeV LHC on the top-Higgs FCNC couplings  $\kappa_{tqh}$  for case (I) – (III). The conjugate processes have been included in the calculations.

In Fig.3, we show the dependence of the cross sections  $\sigma_{thj}$  on the top-Higgs FCNC couplings  $\kappa_{tqh}$  at 8 and 14 TeV LHC respectively for three different cases: (I)  $\kappa_{tqh} = \kappa_{tuh} = \kappa_{tch}$ , (II)  $\kappa_{tqh} = \kappa_{tuh}, \kappa_{tch} = 0$  and (III)  $\kappa_{tqh} = \kappa_{tch}, \kappa_{tuh} = 0$ . For the three cases, the main contribution to  $pp \rightarrow thj$  is from the resonant production  $pp \rightarrow t\bar{t} \rightarrow thj$ . The non-resonant contributions are dominated by the process  $gq \rightarrow thj$ . To be specific, we can have the following observations:

- Case-(I): When  $\kappa_{tqh} = 0.1$ , the total cross section of  $pp \rightarrow thj$  at 8 and 14 TeV LHC can be respectively enhanced up to nearly 176 and 145 times the SM predictions [25].

For the smaller values of  $\kappa_{tqh}$ , the cross section will decrease and become comparable with the SM prediction when  $\kappa_{tqh} \sim 0.008$ . Here it should be mentioned that although the CMS collaboration has performed a search for  $thj$  event at  $\sqrt{s} = 8$  TeV and given a 95% upper limit on the  $thj$  cross section  $\sigma_{thj} < 2.24$  pb, this bound is not suitable for our case because a forward jet with  $|\eta| > 1.0$  is required in the experimental analysis. We can also see that the full cross section of  $pp \rightarrow thj$  is 1.08 (1.06) times larger than the one of  $pp \rightarrow t\bar{t} \rightarrow thj$  at 8 (14) TeV LHC due to the contributions of the non-resonant productions of  $hj$ .

- Case-(II) and (III): For the same values of  $\kappa_{tuh}$  and  $\kappa_{tch}$ , the cross section of  $pp \rightarrow thj$  in case-(II) is much larger than that in case-(III), since the up-quark has the larger PDF than the charm-quark. This feature allows us to separately probe the couplings between  $\kappa_{tuh}$  and  $\kappa_{tch}$  at the LHC. So, in general, for a given collider energy and luminosity, we can expect the sensitivity to the coupling  $\kappa_{tuh}$  will be better than  $\kappa_{tch}$ . It should be also mentioned that the dominant contribution to  $pp \rightarrow thj$  in case-(II) and case-(III) still come from  $gg$ -fusion process. The main difference between case-(II) and case-(III) lies in the contribution of  $qg \rightarrow thj$  process. This makes the complete cross section of  $thj$  almost same as that of  $t\bar{t} \rightarrow thj$  in case-(III) because of the small portion of  $c$  quark in the proton. To be specific, when  $\sqrt{s} = 8(14)$  TeV and  $\kappa_{tqh} = 0.1$ ,  $\sigma_{pp \rightarrow thj}$  is about 1.16(1.12) and 1.006(1.005) times larger than  $\sigma_{pp \rightarrow t\bar{t} \rightarrow thj}$  in case-(II) and -(III), respectively.
- Case-(I) and (II): We also find that the impact of  $qg \rightarrow thj$  on increasing the cross section of  $thj$  production in case-(I) is smaller than that in case-(II). The reason is that the main production mode  $qg \rightarrow thj$  in case-(I) includes both of  $qg \rightarrow th\bar{u}$  and  $qg \rightarrow th\bar{c}$ , while in case-(II) only the former process can contribute to  $qg \rightarrow thj$  production. On the other hand, the cross section of  $qg \rightarrow thj$  is almost same in case-(I) and (II) since it is dominated by the subprocess  $ug \rightarrow thg$ .

In the following calculations, we perform the Monte Carlo simulation and explore the sensitivity of 14 TeV LHC to the top-Higgs FCNC couplings through the channel,

$$pp \rightarrow t(\rightarrow b\ell^+\nu_\ell)h(\rightarrow \gamma\gamma)j, \quad (4)$$

which is characterized by two photons appearing as a narrow resonance centered around the

Higgs boson mass. So the SM backgrounds to the Eq.(4) include two parts: the resonant and the non-resonant backgrounds. For the former, they mainly come from the processes that have a Higgs boson decaying to diphoton in the final states, such as  $Whjj$ ,  $Zhjj$  and  $t\bar{t}h$  productions. The additional jets in the  $Whjj/Zhjj$  events come from the initial or final state radiations. The cross sections of the resonant backgrounds are normalized to their NLO values; For the latter, the main background processes contain the diphoton events produced in association with top quarks, such as  $tj\gamma\gamma$  and  $t\bar{t}\gamma\gamma$ . The  $Wjj\gamma\gamma$  production can also mimic the signal when one light jet is mistagged as a  $b$  jet.

We generate signal and background events with MadGraph5 and perform the parton shower and the fast detector simulations with PYTHIA [39] and Delphes [40]. When generating the parton level events, we assume  $\mu_R = \mu_F$  to be the default event-by-event value. We cluster the jets by setting the anti- $k_t$  algorithm with a cone radius  $\Delta R = 0.5$  [41]. The  $b$ -jet tagging efficiency( $\epsilon_b$ ) is formulated as a function of the transverse momentum and rapidity of the jets [42]. The mis-tag of QCD jets is assumed to be the default value as in Delphes. In our simulation, we generate 100k events for the signals and backgrounds respectively.

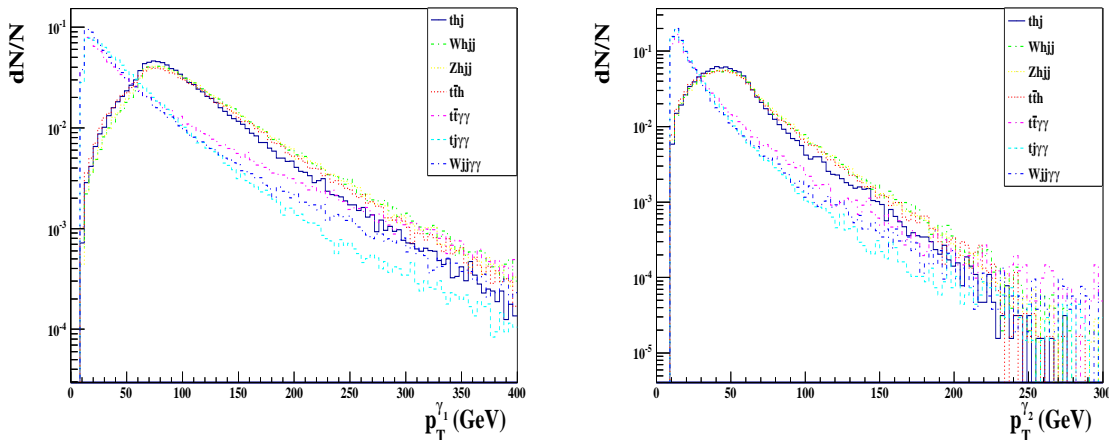


FIG. 4: Normalized transverse momentum distributions of two photons in the signals and backgrounds at 14 TeV LHC.

In Fig.4, we show the transverse momentum distributions of two photons in the signal with  $\kappa_{tqh} = 0.1$  and backgrounds at 14 TeV LHC. Since the two photons in the signal and the resonant backgrounds come from the Higgs boson, they have peaks around  $m_h/2$  and possess the harder  $p_T$  spectrum than those in the non-resonant backgrounds. According to Fig.4, we can impose the cuts  $p_T^{\gamma_1} > 50$  GeV and  $p_T^{\gamma_2} > 25$  GeV to suppress the non-resonant

backgrounds.

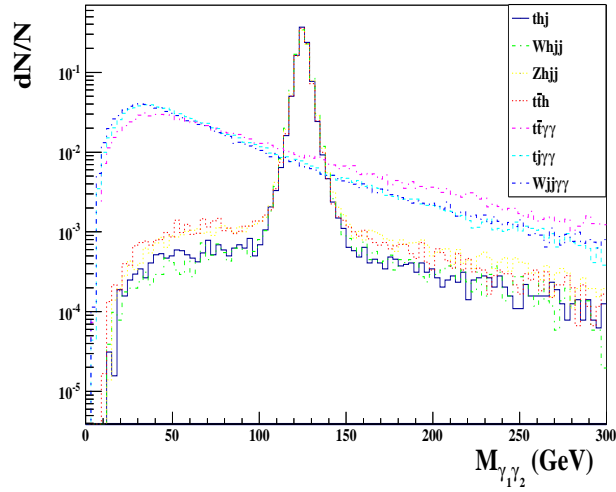


FIG. 5: Normalized invariant mass distribution of two photons at 14 TeV LHC.

In Fig.5, we present the normalized invariant mass distribution of two photons at 14 TeV LHC. Although the  $\gamma\gamma$  decay channel has a small branching ratio, it has the advantage of the good resolution on the  $\gamma\gamma$  resonance and is also free from the large QCD backgrounds. From Fig.5, we can see that the spreading of the  $\gamma\gamma$  invariant-mass peak at  $m_h$  for the signal and the resonant backgrounds is relatively small. We will use a narrow invariant mass window  $|M_{\gamma\gamma} - M_h| < 5$  GeV to further reduce the non-resonant backgrounds.

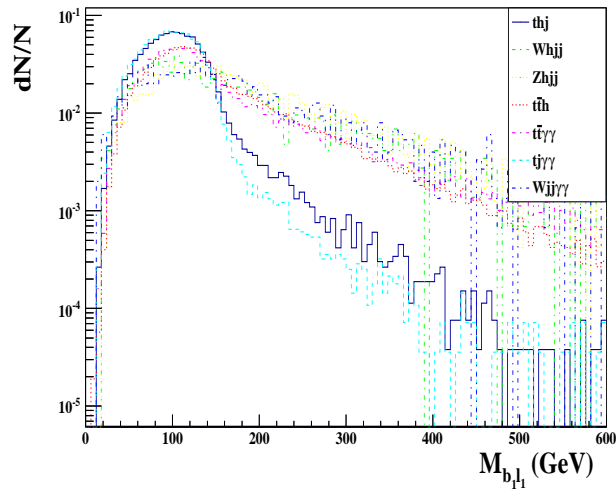


FIG. 6: Normalized invariant mass distribution of the  $b$  jet and lepton at 14 TeV LHC.

In Fig.6, we plot the normalized invariant mass distribution of the  $b$  jet and lepton at



14 TeV LHC, which is another effective cut to remove the backgrounds. From Fig.6, we can see that the invariant mass  $M_{b_1\ell_1}$  of the signal is always less than the top quark mass since the leading  $b$  jet and lepton in our signal come from the same top quark decay. The same feature also appears in the non-resonant background  $tj\gamma\gamma$ . But other backgrounds can have higher invariant mass  $M_{b_1\ell_1}$  than the signal. Very similar to  $M_{b_1\ell_1}$ , the invariant mass distribution of the diphoton and leading light jet  $M_{\gamma_1\gamma_2j}$  also has a peak around the top quark mass in the signal other than the backgrounds, which can be used to further remove the backgrounds.

TABLE I: Cut flow of the cross sections for the backgrounds and the signals in the Case-(I), (II) and (III) at 14 TeV LHC, where  $\kappa_{tqh}$ ,  $\kappa_{tuh}$  and  $\kappa_{tch}$  are assumed to be 0.1 respectively and the symbol "—" stands for the events number less than one. As a comparison, the corresponding results of the resonant production  $pp \rightarrow t\bar{t} \rightarrow thj$  for each case are also listed in the table.

Cuts	Cross sections ( $10^{-3} \text{ fb}^{-1}$ )							
	$thj(t\bar{t})$			$t\bar{t}h$	$Vhj$	$t\bar{t}\gamma\gamma$	$tj\gamma\gamma$	$Wjj\gamma\gamma$
	Case-I	Case-II	Case-III					
(1) $\Delta R_{ij} > 0.4, \quad i, j = b, j, \gamma \text{ or } \ell$ $p_T^b > 25 \text{ GeV}, \quad  \eta_b  < 2.5$ $p_T^\ell > 20 \text{ GeV}, \quad  \eta_\ell  < 2.0$ $p_T^j > 25 \text{ GeV}, \quad  \eta_j  < 2.5$	2.51(2.32)	1.35(1.16)	1.16(1.16)	0.035	0.08	4.05	2.92	2.13
(2) $p_T^{\gamma_1} > 50 \text{ GeV}, p_T^{\gamma_2} > 25 \text{ GeV}$	2.27(2.10)	1.22(1.05)	1.05(1.05)	0.032	0.007	1.91	1.50	1.28
(3) $M_{b_1\ell_1} < 200 \text{ GeV}$	2.27(2.10)	1.22(1.05)	1.05(1.05)	0.030	0.005	1.77	1.48	0.85
(4) $ M_{\gamma_1\gamma_2} - m_h  < 5 \text{ GeV}$	1.99(1.86)	1.06(0.93)	0.93(0.93)	0.022	0.004	0.07	0.09	-
(5) $M_{\gamma_1\gamma_2j_1} < 300 \text{ GeV}$	1.54(1.46)	0.81(0.73)	0.73(0.73)	0.01	0.002	-	0.07	-

According to the above analysis, events are selected to satisfy the following criteria:

- exact one isolated lepton with  $p_T(\ell_1) > 20 \text{ GeV}$  and  $|\eta_{\ell_1}| < 2$ .
- a hard jet with  $p_T(j_1) > 25 \text{ GeV}$  and  $|\eta_{j_1}| < 2.5$  and one  $b$ -jet with  $p_T(b_1) > 25 \text{ GeV}$  and  $|\eta_{b_1}| < 2.5$ ;
- two photons with  $p_T^{\gamma_1} > 50 \text{ GeV}$  and  $p_T^{\gamma_2} > 25 \text{ GeV}$  and their invariant mass  $M_{\gamma_1\gamma_2}$  in the range of  $M_h \pm 5 \text{ GeV}$ ;
- the invariant mass of  $b$ -jet and lepton  $M_{b\ell} < 200 \text{ GeV}$
- the invariant mass of diphoton and leading jet  $M_{\gamma_1\gamma_2j_1} < 300 \text{ GeV}$ .

In Table I, we give the cross sections of the signals in the Case-(*I*), (*II*) and (*III*) and backgrounds after the cut flow at 14 TeV LHC, where  $\kappa_{tqh}$ ,  $\kappa_{tuh}$  and  $\kappa_{tch}$  are assumed to be 0.1 respectively. From Table I, we can see that all the non-resonant backgrounds after the cuts of the two photons are reduced by half while the signals and the resonant backgrounds are hurt slightly. Then, we impose the invariant mass cut  $M_{b_1\ell_1} < 200$  GeV to remove the backgrounds that do not involve the top quark. Since the photon final states have a good energy resolution in the detector, we require that  $M_{\gamma_1\gamma_2}$  be in the range of  $120\text{GeV} < M_{\gamma_1\gamma_2} < 130\text{GeV}$  and  $M_{\gamma_1\gamma_2j_1} < 300$  GeV, which can further suppress the backgrounds by half. So at the end of the cut flow, the largest background is  $tj\gamma\gamma$ , which is followed by  $t\bar{t}h$ .

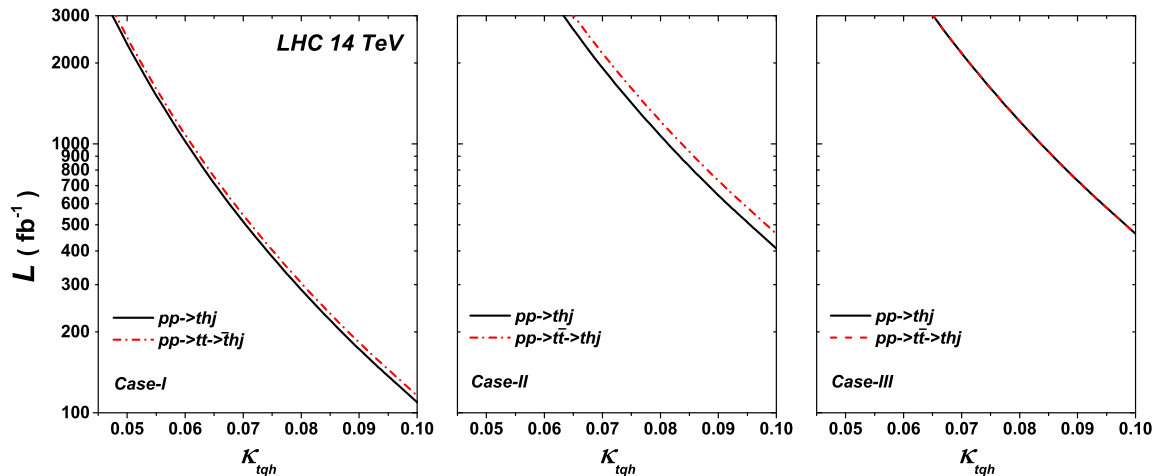


FIG. 7: Contour plots in  $\mathcal{L} - \kappa_{tqh}$  plane for statistical significance  $S/\sqrt{B} = 3\sigma$  of  $pp \rightarrow thj$  at 14 TeV LHC. The conjugate processes have been included in the calculations. The cross section of  $t\bar{t}$  is normalized to the approximately next-to-next-to-leading order value  $\sigma_{t\bar{t}} = 920$  pb [43]. As a comparison, the corresponding results of the resonant production  $pp \rightarrow t\bar{t} \rightarrow thj$  for each case are also displayed.

In Fig.7, we plot the contours of statistical significance  $S/\sqrt{B} = 3\sigma$  of  $pp \rightarrow thj$  at 14 TeV LHC for the Case-(*I*), (*II*) and (*III*) in the plane of  $\mathcal{L} - \kappa_{tqh}$ . From Fig.7, we can see that the flavor changing couplings  $\kappa_{tqh}$  can be probed to 0.047, 0.063 and 0.065 at  $3\sigma$  statistical sensitivity by fully calculating the production of  $thj$  for the case (*I*), (*II*) and (*III*) respectively, which correspond to the branching ratios  $Br(t \rightarrow qh) = 0.12\%$ ,  $Br(t \rightarrow uh) = 0.23\%$  and  $Br(t \rightarrow ch) = 0.26\%$  at 14 TeV LHC with  $\mathcal{L} = 3000 \text{ fb}^{-1}$ . Besides, the corresponding results of the resonant production  $pp \rightarrow t\bar{t} \rightarrow thj$  for each case

are also displayed. We can see that the LHC sensitivity to the coupling  $\kappa_{tqh}$  from the full calculation of  $thj$  production in the Case-(II) can be improved by about 4% as a comparison with the resonant production  $pp \rightarrow t\bar{t} \rightarrow thj$ , while for other two cases, the enhancement is negligible small. Here it should be mentioned that we normalize the leading order cross section of  $t\bar{t}$  to the approximately next-to-next-to-leading order value  $\sigma_{t\bar{t}} = 920$  pb [43]. But the contribution of  $qg \rightarrow thj$  is calculated at the leading order due to lack of the high order correction. So if assuming that the  $k$  factor of the process  $qg \rightarrow thj$  be the same as  $t\bar{t}$ , we can expect the sensitivity to the coupling  $\kappa_{tqh}$  from full calculation in Case-(I) and (II) will be further increased. Compared with other decay modes of the Higgs boson, our result is close to that of multi-leptons channel in  $t\bar{t} \rightarrow th(\rightarrow WW^*, \tau^+\tau^-, ZZ^*)j$  production [44], based native scaling in cross section and luminosity at 14 TeV LHC. Although the decay of  $h \rightarrow b\bar{b}$  has a larger branching ratio and seems more promising [22], the analysis was performed at the parton level without including the parton shower and detector effects. However, these effects are important for the Higgs mass reconstruction and can severely reduce the cut efficiency of Higgs mass window in  $b\bar{b}$  channel.

#### IV. CONCLUSION

In the work, we investigated the process  $pp \rightarrow thj$  induced by the top-Higgs FCNC couplings at the LHC. We found that the cross section of  $pp \rightarrow thj$  can be sizably enhanced in contrast with the SM predictions at 8 and 14 TeV LHC under the current constraints. We studied the observability of top-Higgs FCNC couplings through the process  $pp \rightarrow t(\rightarrow b\ell^+\nu_\ell)h(\rightarrow \gamma\gamma)j$  by including the resonant and non-resonant  $hj$  production at 14 TeV LHC. Compared with the resonant production  $pp \rightarrow t\bar{t} \rightarrow thj$ , such a full calculation can increase the LHC  $3\sigma$  sensitivity to  $Br(t \rightarrow qh)$  by 4% and  $Br(t \rightarrow uh)$  by 10% at 14 TeV LHC with  $\mathcal{L} = 3000$  fb $^{-1}$  because of the contribution of the non-resonant production  $qg \rightarrow thj$ . Finally, the branching ratios  $Br(t \rightarrow qh)$ ,  $Br(t \rightarrow uh)$  and  $Br(t \rightarrow ch)$  can be respectively probed to 0.12%, 0.23% and 0.26% at  $3\sigma$  level at 14 TeV LHC with  $\mathcal{L} = 3000$  fb $^{-1}$ .

## Acknowledgement

This work was supported by the Australian Research Council, the National Natural Science Foundation of China (NNSFC) under grants Nos. 11275057, 11305049 and 11405047, by Specialized Research Fund for the Doctoral Program of Higher Education under Grant No.20134104120002.

- 
- [1] G. Aad et al.(ATLAS Collaboration), Phys. Lett. B **710**, 49 (2012).
  - [2] S. Chatrchyan et al.(CMS Collaboration), Phys. Lett. B **710**, 26 (2012).
  - [3] the recent reviews, see examples: S. Dawson, A. Gribsan, H. Logan, J. Qian, C. Tully, R. Van Kooten, A. Ajaib and A. Anastassov *et al.*, arXiv:1310.8361 [hep-ex]; C. Englert, A. Freitas, M. Muhlleitner, T. Plehn, M. Rauch, M. Spira and K. Walz, arXiv:1403.7191 [hep-ph];
  - [4] For top quark reviews, see, e.g., C. S. Li, H. T. Li and D. Y. Shao, arXiv:1401.1101 [hep-ph]; K. Agashe *et al.* [Top Quark Working Group Collaboration], arXiv:1311.2028 [hep-ph]; C. Zhang and S. Willenbrock, Nuovo Cim. C **033**, no. 4, 285 (2010) [arXiv:1008.3155 [hep-ph]]; W. Bernreuther, J. Phys. G **35**, 083001 (2008) [arXiv:0805.1333 [hep-ph]]; J. A. Aguilar-Saavedra, Nucl. Phys. B **812**, 181 (2009) [arXiv:0811.3842 [hep-ph]]; Nucl. Phys. B **821**, 215 (2009) [arXiv:0904.2387 [hep-ph]]; E. W. N. Glover, *et al.*, Acta Phys. Polon. B **35**, 2671 (2004) [hep-ph/0410110]; D. Chakraborty, J. Konigsberg and D. L. Rainwater, Ann. Rev. Nucl. Part. Sci. **53**, 301 (2003) [hep-ph/0303092]; M. Beneke, *et al.*, hep-ph/0003033; T. Han, Int. J. Mod. Phys. A **23**, 4107 (2008) [arXiv:0804.3178 [hep-ph]];
  - [5] G. Eilam, J. L. Hewett, A. Soni, Phys. Rev. D **44**, 1473 (1991); B. Mele, S. Petrarca, A. Soddu, Phys. Lett. B **435**, 401 (1998); A. Cordero-Cid *et al.*, Phys. Rev. D **73**, 094005 (2006); G. Eilam, M. Frank, I. Turan, Phys. Rev. D **73**, 053011 (2006).
  - [6] J. Cao, C. Han, L. Wu, J. M. Yang and M. Zhang, arXiv:1404.1241 [hep-ph]. T. -J. Gao, T. -F. Feng, F. Sun, H. -B. Zhang and S. -M. Zhao, arXiv:1404.3289 [hep-ph]; S. Bejar, J. Guasch, D. Lopez-Val and J. Sola, Phys. Lett. B **668**, 364 (2008) [arXiv:0805.0973 [hep-ph]]; J. Cao *et al.*, Phys. Rev. D **75**, 075021 (2007); M. Frank and I. Turan, Phys. Rev. D **74**, 073014 (2006); S. Bejar, J. Guasch and J. Sola, JHEP **0510**, 113 (2005) [hep-ph/0508043]; J. L. Diaz-Cruz, H.-J. He, C.-P. Yuan Phys. Lett. B **179**,530 (2002); J. Guasch and J. Sola, Nucl. Phys. B **562**,

- 3 (1999); C. S. Li, R. J. Oakes and J. M. Yang, Phys. Rev. D **49**, 293 (1994); J. M. Yang and C. S. Li, Phys. Rev. D **49**, 3412 (1994);
- [7] Z. -x. Heng, G. -r. Lu, L. Wu and J. M. Yang, Phys. Rev. D **79**, 094029 (2009) [arXiv:0904.0597 [hep-ph]]; J. Cao, Z. Heng, L. Wu and J. M. Yang, Phys. Rev. D **79**, 054003 (2009) [arXiv:0812.1698 [hep-ph]]; J. M. Yang, B.-L. Young and X. Zhang, Phys. Rev. D **58**, 055001 (1998); G. Eilam *et al.*, Phys. Lett. B **510**, 227 (2001).
- [8] T. Han and R. Ruiz, Phys. Rev. D **89**, 074045 (2014) [arXiv:1312.3324 [hep-ph]]; K. -F. Chen, W. -S. Hou, C. Kao and M. Kohda, Phys. Lett. B **725**, 378 (2013) [arXiv:1304.8037 [hep-ph]]; C. Kao, H. -Y. Cheng, W. -S. Hou and J. Sayre, Phys. Lett. B **716**, 225 (2012) [arXiv:1112.1707 [hep-ph]]; A. Arhrib, K. Cheung, C. W. Chiang and T. C. Yuan, Phys. Rev. D **73**, 075015 (2006); M. Frank and I. Turan, Phys. Rev. D **72**, 035008 (2005); J. A. Aguilar-Saavedra, B. M. Nobre, Phys. Lett. B **553**, 251 (2003); E. O. Iltan and I. Turan Phys. Rev. D **67**, 015004 (2003); S. Bejar, J. Guasch and J. Sola, Nucl. Phys. B **600**, 21 (2001); F. del Aguila, J. A. Aguilar-Saavedra, R. Miquel, Phys. Rev. Lett. **82**, 1628 (1999); S. Bar-Shalom *et al.*, Phys. Rev. Lett. **79**, 1217(1997); W. S. Hou, G.-L. Lin and C.-Y. Ma, Phys. Rev. D **56**, 7434(1997); J. L. Diaz-Cruz *et al.* Phys. Rev. D **41**, 891(1990).
- [9] D. Atwood, L. Reina and A. Soni, Phys. Rev. D **55**, 3156 (1997) [hep-ph/9609279];
- [10] B. Yang, N. Liu and J. Han, arXiv:1308.4852 [hep-ph]. L. Wang, L. Wu and J. M. Yang, Phys. Rev. D **85**, 075017 (2012) [arXiv:1111.4771 [hep-ph]]; J. Cao, K. Hikasa, L. Wang, L. Wu and J. M. Yang, Phys. Rev. D **85**, 014025 (2012) [arXiv:1109.6543 [hep-ph]]; G. Liu and H. -j. Zhang, arXiv:0708.1553 [hep-ph].
- [11] M. Gorbahn and U. Haisch, JHEP **1406**, 033 (2014) [arXiv:1404.4873 [hep-ph]]; C. -X. Yue, S. -Y. Cao and Q. -G. Zeng, JHEP **1404**, 170 (2014) [arXiv:1401.5159 [hep-ph]]; C. Han, N. Liu, L. Wu and J. M. Yang, Phys. Lett. B **714**, 295 (2012) [arXiv:1203.2321 [hep-ph]]; J. Cao, L. Wu and J. M. Yang, Phys. Rev. D **83**, 034024 (2011) [arXiv:1011.5564 [hep-ph]]; G. -R. Lu and L. Wu, Chin. Phys. Lett. **27**, 031401 (2010). J. Drobnak, S. Fajfer and J. F. Kamenik, JHEP **0903**, 077 (2009) [arXiv:0812.0294 [hep-ph]]. J. Cao, Z. Xiong and J. M. Yang, Nucl. Phys. B **651**, 87 (2003);
- [12] J. Cao, L. Wang, L. Wu and J. M. Yang, Phys. Rev. D **84**, 074001 (2011) [arXiv:1101.4456 [hep-ph]]; J. Cao, Z. Heng, L. Wu and J. M. Yang, Phys. Rev. D **81**, 014016 (2010) [arXiv:0912.1447 [hep-ph]]; A. Azatov, M. Toharia and L. Zhu, Phys. Rev. D **80**, 035016

- (2009) [arXiv:0906.1990 [hep-ph]]; K. Agashe and R. Contino, Phys. Rev. D **80**, 075016 (2009) [arXiv:0906.1542 [hep-ph]].
- [13] For reviews on top FCNC processes in new physics models, see, e.g., P. M. Ferreira, R. B. Guedes and R. Santos, Phys. Rev. D **77**, 114008 (2008) [arXiv:0802.2075 [hep-ph]]; F. Larios, R. Martinez, M. A. Perez, Int. J. Mod. Phys. A **21**, 3473 (2006); J. M. Yang, Annals Phys. **316**, 529 (2005); J. A. Aguilar-Saavedra, Acta Phys. Polon. B **35**, 2695 (2004) [hep-ph/0409342].
- [14] E. Yazgan [ATLAS and CDF and CMS and D0 Collaborations], arXiv:1312.5435 [hep-ex].
- [15] G. Aad *et al.* [ATLAS Collaboration], JHEP **1406**, 008 (2014) [arXiv:1403.6293 [hep-ex]].
- [16] [CMS Collaboration], CMS-PAS-HIG-13-034.
- [17] A. Greljo, J. F. Kamenik and J. Kopp, JHEP **1407**, 046 (2014) [arXiv:1404.1278 [hep-ph]].
- [18] S. Khatibi and M. M. Najafabadi, Phys. Rev. D **89**, 054011 (2014) [arXiv:1402.3073 [hep-ph]].
- [19] D. Atwood, S. K. Gupta and A. Soni, arXiv:1305.2427 [hep-ph].
- [20] Y. Wang, F. P. Huang, C. S. Li, B. H. Li, D. Y. Shao and J. Wang, Phys. Rev. D **86**, 094014 (2012) [arXiv:1208.2902 [hep-ph]].
- [21] D. Lopez-Val, J. Guasch and J. Sola, JHEP **0712**, 054 (2007) [arXiv:0710.0587 [hep-ph]].
- [22] J. A. Aguilar-Saavedra and G. C. Branco, Phys. Lett. B **495**, 347 (2000) [hep-ph/0004190].
- [23] T. M. P. Tait and C.-P. Yuan, Phys. Rev. D **63**, 014018 (2000) [hep-ph/0007298].
- [24] F. Maltoni, K. Paul, T. Stelzer and S. Willenbrock, Phys. Rev. D **64**, 094023 (2001) [hep-ph/0106293].
- [25] M. Farina, C. Grojean, F. Maltoni, E. Salvioni and A. Thamm, JHEP **1305**, 022 (2013) [arXiv:1211.3736 [hep-ph]].
- [26] S. Biswas, E. Gabrielli and B. Mele, JHEP **1301**, 088 (2013) [arXiv:1211.0499 [hep-ph]].
- [27] J. Ellis, D. S. Hwang, K. Sakurai and M. Takeuchi, JHEP **1404**, 004 (2014) [arXiv:1312.5736 [hep-ph]].
- [28] C. Englert and E. Re, Phys. Rev. D **89**, 073020 (2014) [arXiv:1402.0445 [hep-ph]].
- [29] J. Chang, K. Cheung, J. S. Lee and C. -T. Lu, JHEP **1405**, 062 (2014) [arXiv:1403.2053 [hep-ph]].
- [30] A. Kobakhidze, L. Wu and J. Yue, arXiv:1406.1961 [hep-ph].
- [31] C. S. Li, R. J. Oakes and T. C. Yuan, Phys. Rev. D **43**, 3759 (1991).
- [32] C. Zhang and F. Maltoni, Phys. Rev. D **88**, 054005 (2013) [arXiv:1305.7386 [hep-ph]]; J. Drob-

- nak, S. Fajfer and J. F. Kamenik, Phys. Rev. Lett. **104**, 252001 (2010) [arXiv:1004.0620 [hep-ph]]; J. J. Zhang, C. S. Li, J. Gao, H. Zhang, Z. Li, C. -P. Yuan and T. -C. Yuan, Phys. Rev. Lett. **102**, 072001 (2009) [arXiv:0810.3889 [hep-ph]].
- [33] J. Cao *et al.*, Phys. Rev. D **74**, 031701 (2006).
- [34] G. C. Branco, W. Grimus and L. Lavoura, Phys. Lett. B **380**, 119 (1996); [hep-ph/9601383]; A. S. Joshipura and S. D. Rindani, Phys. Lett. B **260**, 149 (1991); T. P. Cheng and M. Sher, Phys. Rev. D **35**, 3484 (1987).
- [35] A. Alloul, N. D. Christensen, C. Degrande, C. Duhr and B. Fuks, arXiv:1310.1921 [hep-ph].
- [36] J. Alwall *et al.*, JHEP **1106**, 128 (2011).
- [37] J. Pumplin *et al.*, JHEP **0602**, 032 (2006).
- [38] J. Beringer *et al.*, Particle Data Group, Phys. Rev. D **86**, 010001 (2012).
- [39] T. Sjostrand, S. Mrenna and P. Z. Skands, JHEP **0605**, 026 (2006).
- [40] J. de Favereau, *et al.*, arXiv:1307.6346 [hep-ex].
- [41] M. Cacciari, G. P. Salam and G. Soyez, JHEP **0804**, 063 (2008).
- [42] CMS Collaboration, b-Jet Identification in the CMS Experiment, CMS-PAS-BTV-11-004.
- [43] N. Kidonakis Phys. Rev. D **84**, 011504(2011).
- [44] N. Craig, J. A. Evans, R. Gray, M. Park, S. Somalwar, S. Thomas and M. Walker, Phys. Rev. D **86**, 075002 (2012) [arXiv:1207.6794 [hep-ph]].